

Radiative charge transfer in collisions of C with He⁺

James F Babb¹†, and B M McLaughlin^{1,2}||

¹Institute for Theoretical Atomic and Molecular Physics, Harvard Smithsonian Center for Astrophysics, MS-14, Cambridge, MA 02138, USA

²Centre for Theoretical Atomic, Molecular and Optical Physics (CTAMOP), School of Mathematics and Physics, The David Bates Building, 7 College Park, Queen's University Belfast, Belfast BT7 1NN, UK

Abstract. Radiative charge exchange collisions between a carbon atom C(³P) and a helium ion He⁺(²S), both in their ground state, are investigated theoretically. Detailed quantum chemistry calculations are carried out to obtain potential energy curves and transition dipole matrix elements for doublet and quartet molecular states of the HeC⁺ cation. Radiative charge transfer cross sections and rate coefficients are calculated and are found at thermal and lower energies to be large compared to those for direct charge transfer. The present results might be applicable to modelling the complex interplay of [C II] (or C⁺), C, and CO at the boundaries of interstellar photon dominated regions (PDRs) and in xray dominated regions (XDRs), where the abundance of He⁺ affects the abundance of CO.

PACS numbers: 31.15.A, 31.15.ae, 34.50 Cx, 34.70.+e

Short title: Radiative charge transfer in collisions of C with He⁺

† E-mail: jbabb@cfa.harvard.edu

|| E-mail: bmclaughlin899@btinternet.com

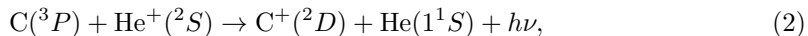
1. Introduction

Models of carbon monoxide formation in the ejecta of supernova SN 1987a were found to be sensitive to the description of charge transfer collisions between metal atoms and He⁺, but corresponding charge transfer rate coefficients were estimated due to the unavailability of measured or calculated values [1, 2]. To remove this uncertainty, charge transfer cross sections and rate coefficients were calculated for C + He⁺ [3, 4] and for O + He⁺ [5, 6]. However, according to the results from this early work, the calculated values were found to be too small to affect appreciably the conclusions reached in the modelling studies.

We note that in the most recent study on O + He⁺, Zhao and co-workers [6] found that the radiative charge exchange process was more significant compared to the nonradiative charge exchange (or direct charge exchange) process. The dominant channel is that which leaves the O⁺ ion in its ground state, namely,



where $h\nu$ is the photon energy [6]. Earlier studies on C + He⁺, by Kimura and co-workers [4], concluded that nonradiative charge exchange was the dominant process in comparison to radiative charge exchange which leaves the C⁺ in the excited ²D state,



though they did not consider the channel—analogue to (1)—where the carbon ion exits in its ground state,



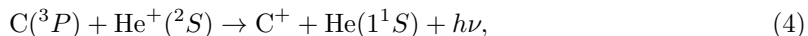
In this paper, we reconsider the radiative charge exchange process for C and He⁺(²S), extending the final states to C⁺(²P^o) and C⁺(⁴P). We find—similarly to O + He⁺—that radiative charge exchange (3) is considerably larger than direct charge exchange at thermal and lower collisional energies.

The layout of this paper is as follows. In section 2 we present the theoretical methods used to calculate the cross sections and rates. Section 3 presents the results from our work and provides a discussion of our results. Finally in section 4, conclusions are drawn from our work, and we briefly consider implications of these, and other recent results, for metal atoms in charge exchange collisions with He⁺ for astrophysical modelling.

2. Theory

2.1. Molecular Structure

We consider the reaction,



representing a collision between a C(³P) atom and a He⁺(²S) ion, which via an electric dipole radiative transition, results in a residual C⁺ ion being left in one of the final states; ²P^o, ⁴P, ²D, ²S or ²P. Relative to the energy of the initial colliding atom ion pair C(³P) + He⁺(²S), the ²P state is slightly above (0.39 eV) the entrance energy, while the ²P^o state lies lower (−13.33 eV) compared to the ²S (−1.37 eV), ²D state (−4.04 eV), and ⁴P state (−8.00 eV). The possible molecular states formed corresponding to the initial C(³P) + He⁺(²S) reactants and the final C⁺ + He(1¹S) residual products are listed in Table 1.

Table 1. The HeC⁺ cation separated atom ion pair potential energies at an interatomic distance of $R=12 a_0$, compared to the energies at asymptotically large internuclear distance from the NIST tabulations [7]. The left pointing arrows mark the entrance channels for the atom ion colliding pair. The Bohr radius a_0 is $5.291\,772\,106\,7 \times 10^{-9}$ cm. All energies are given in eV.

Separated Atom Ion Pair	Molecular States	Energy (eV) ^a ($R=12 a_0$)	Energy (eV) ^b ($R \rightarrow \infty$)
He(1^1S) + C ⁺ ($2P$)	$4^2\Pi$, $2^2\Sigma^-$	13.64	13.72
← He ⁺ ($2S$) + C($3P$)	← $2^4\Sigma^-$	13.50	13.33
	← $2^4\Pi$	13.47	13.33
	← $3^2\Pi$	13.24	13.33
	← $D^2\Sigma^-$	13.23	13.33
He(1^1S) + C ⁺ ($2S$)	$3^2\Sigma^+$	11.95	11.96
He(1^1S) + C ⁺ ($2D$)	$C^2\Delta$, $2^2\Sigma^+$, $B^2\Pi$	9.22	9.29
He(1^1S) + C ⁺ ($4P$)	$b^4\Pi$	5.33	5.33
	$a^4\Sigma^-$	5.32	5.33
He(1^1S) + C ⁺ ($2P^o$)	$X^2\Pi$, $A^2\Sigma^+$	0.00	0.00

^aPresent MOLPRO MRCI+Q calculations.

^bNIST tabulations, Kramida *et al.* [7].

The $X^2\Pi$, $A^2\Sigma^+$, $a^4\Sigma^-$, and $b^4\Pi$ potential energy curves (PECs) were calculated by Matoba *et al* [8] and by Tuttle *et al* [9], who presented a critical summary of earlier calculations. Kimura and co-workers [3] calculated the PECs of the $D^2\Sigma^-$ and $B^2\Pi$ states and they extended these calculations to include the PECs of the $C^2\Delta$, $3^2\Pi$, $4^2\Pi$, and $2^2\Sigma^-$ states and the transition dipole moment (TDM) between the $3^2\Pi$ and $B^2\Pi$ states [4].

Since a complete set of PECs and TDMs is not available in the literature, for the present study we calculated the molecular data for all the states listed in Table 1. A brief summary of our structure calculations is provided below. In our molecular structure work we used a state-averaged-multi-configuration-self-consistent-field (SA-MCSCF) approach, followed by multi-reference configuration interaction (MRCI) calculations together with the Davidson correction (MRCI+Q) [10]. The SA-MCSCF method is used as the reference wave function for the MRCI calculations. We used augmented correlation consistent polarised aug-cc-pV6Z (AV6Z) basis sets [11–13] in our work as these are known to recover approximately 98% of the electron correlation effects [10] in structure calculations. All the PEC and TDM calculations were performed with the quantum chemistry MOLPRO 2015.1 program package [14], running on parallel architectures. The PECs and TDM calculations were performed on this system from $1.5 a_0$ to an internuclear bond distance of $12 a_0$, beyond which they were matched to their long range form for dynamical calculations.

In MOLPRO the calculations are carried out in C_{2v} symmetry with the order of Abelian irreducible representations being (A_1 , B_1 , B_2 , A_2). In reducing the symmetry from $C_{\infty v}$ to C_{2v} , the correlating relationships are $\sigma \rightarrow a_1$, $\pi \rightarrow (b_1, b_2)$, and $\delta \rightarrow (a_1, a_2)$. In order to take account of short-range interactions we employed the non-relativistic state-averaged complete-active-space-self-consistent-field (SA-CASSCF)/MRCI method [15, 16] available within the MOLPRO quantum

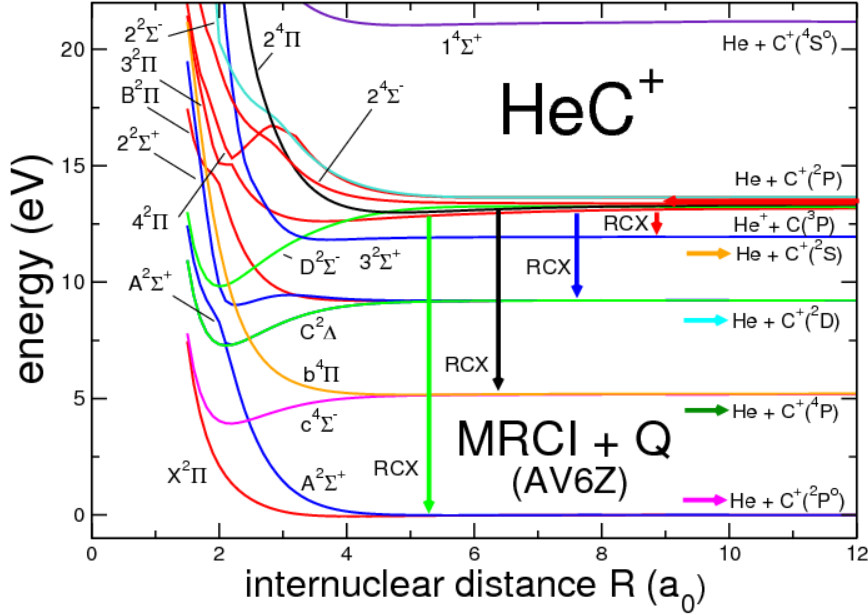


Figure 1. Potential energies for the HeC⁺ molecular ion, as a function of the internuclear distance R (a_0), corresponding to the initial channel $C(^3P)+He^+(^2S)$ and to the final channels of $C^+ + He(1^1S)$. The downward pointing arrows mark the radiative charge exchange (RCX) processes for the dominant doublet and quartet transitions studied here.

chemistry codes. In detail, for this cation, six molecular orbitals (MOs) are put into the active space, including four a_1 , one b_1 and one b_2 symmetry MO's and the 1σ orbital is frozen. The molecular orbitals for the MRCI procedure are obtained from the state-averaged-multi-configuration-self-consistent-field (SA-MCSF) method, where the averaging processes for the doublets is carried out on the lowest six (2A_1), six (2B_1), and five (2A_2) molecular states of this molecule in C_{2v} . Separate calculations were carried out for the case of the quartets, with the same basis set, where the averaging process in this case was performed over the lowest two (4A_1), two (4B_1), and two (4A_2) molecular states of this cation.

These MOs ($4a_1, 1b_1, 1b_2, 0a_2$), denoted by (4,1,1,0), were generated from the state-averaging CASSCF process, and used to perform all the subsequent PEC calculations for all the electronic states in the MRCI+Q approximation. Fig. 1 shows the calculated PECs for the doublet and quartet states of the HeC⁺ cation as a function of bond separation. The TDMs considered in the present work are shown in Fig. 2. A more extensive report on the calculated PECs and TDMs will be presented in a future publication.

For the ground state of the HeC⁺ cation, we find from our calculations that the dissociation energy D_e , of the X²Π state is 62 meV, with equilibrium bond distance

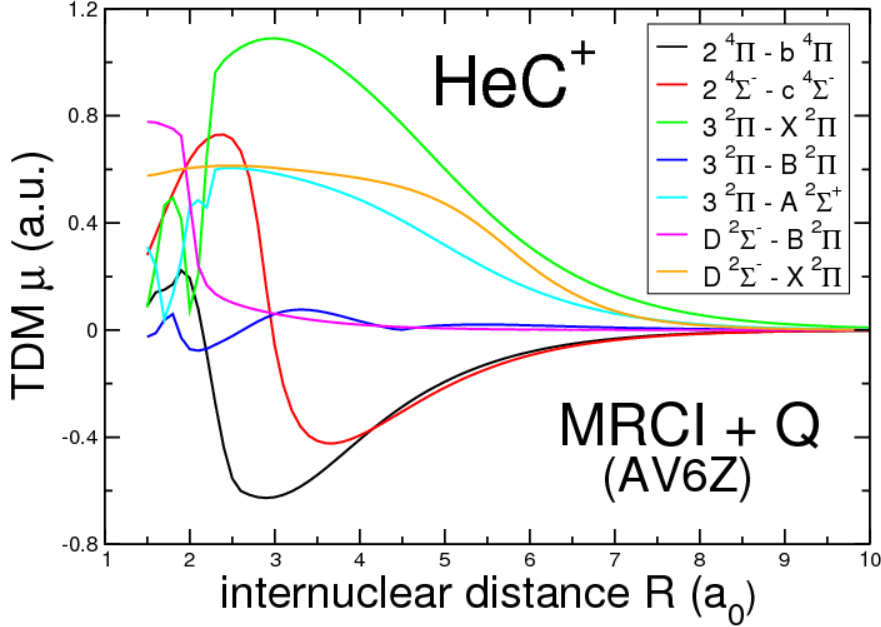


Figure 2. Transition dipole moments, in atomic units, as a function of the internuclear distance R (a_0), for the HeC^+ molecular ion corresponding to the initial channel $\text{C}(^3P) + \text{He}^+(^2S)$ and to the final channel $\text{C}^+(^2P^o) + \text{He}(^1S)$. Illustrated are a sample of dominant transitions studied here for the radiative charge exchange processes (RCX).

$r_e=4.10 a_0$. This is to be compared to earlier values of $D_e=50.34$ meV and $r_e = 4.24 a_0$ obtained by Grice *et al* [17], using the GAUSSIAN 82 quantum chemistry package at the MP4SDQ/6-311 + G(3df,3pd) level of theory, excluding core contributions to the correlation energy. More recent results from higher level approximations give values of $D_e=58.07$ meV and of $r_e=4.18 a_0$, which were obtained by Matoba *et al* [8], with a diffuse aug-cc-pVQZ basis (diffuse AVQZ), within the MCSCF/MRCI approximation using the IBM ALCHEMY II quantum chemistry codes. A value of $D_e=59.03$ meV and $r_e=4.16 a_0$ was found by Tuttle *et al* [9], using the RCCSD(T) approximation, within the MOLPRO quantum chemistry package, and basis sets of quadruple- ζ (AVQZ) and quintuple- ζ (AV5Z) quality; with each point counterpoise corrected and extrapolated to the basis set limit. Our calculations are in good agreement with these recent findings. The value for the dissociation energy D_e is within 7% of the value obtained by Matoba *et al* [8] and within 5% of the more sophisticated calculations of Tuttle *et al* [9]. This is in quite satisfactory agreement for the present study of collisions at thermal energies between this atom ion pair.

To carry out the dynamical cross section calculations for radiative loss, we interpolated the *ab initio* calculated PECs and TDMs using cubic splines. For $R < 1.5 a_0$, the *ab initio* PEC data were connected to the analytic form $a \exp(bR)$, where a

and b for each state were determined by fitting. For $R > 12 a_0$, the appropriate long-range forms were used for the separating atom ion pair. In particular, for $C(^3P) + He(^2S)$, this corresponds to a $Q_{C;\pm}R^{-3}$ quadrupole interaction [18] added to the attractive polarisation potential $-\frac{1}{2}\alpha_C R^{-4}$, where α_C is the $C(^3P)$ atom electric dipole polarisability. The value of Q_C is positive for the $3^2\Pi$ state and negative for the $D^2\Sigma^-$ state, which can be confirmed by close inspection of Fig. 1. The value of α_C also depends on the state of the C atom. Both Allison and co-workers [19] and Miller and Kelly [20] found that the value of the polarisability is about 10 % larger for the $|m_L| = 1$ state of C, compared to the $m_L = 0$ state, though the values from each publication differ. To model the $|m_L| = 1$ polarisability, we increased the $m_L = 0$ polarisability by ten percent [19, 20]. For the $C^+ + He(1^1S)$ system, the long-range form is $-\frac{1}{2}\alpha_{He}R^{-4}$, where α_{He} is the $He(1^1S)$ polarisability.

In carrying out the dynamical cross-section calculations, we fix the potential energies at asymptotically large distances to the values listed in Table 1. To expedite continuity of the TDMs for $R < 1.5 a_0$ we linearly extrapolated to the intercept at $R = 0$. In practice, this region of the TDMs does not affect the calculations detailed below, because the PECs are repulsive and the TDMs are relatively small, as can be seen by inspection of Figs. 1 and 2. The range of internuclear distances, roughly, between 2 and 6 a_0 is most important for the transition amplitudes, see, for example, Fig. 3 of Ref. [4]. For $R > 12 a_0$ we fitted the values to the form R^{-n} , selecting a value of $n \geq 3$.

2.2. Dynamics

We assume the initial channel is $C(^3P) + He(^2S)$. Then, there are a number of allowed electric dipole electronic transitions originating in the $3^2\Pi$ or $D^2\Sigma^-$ initial states to doublet states of lower energy, and similarly for the initial $2^4\Sigma^-$ or $2^4\Pi$ states to quartet states of lower energy.

For HeC^+ , the $X^2\Pi$ and $A^2\Sigma^+$ states are strongly repulsive and molecular ion formation by radiative association will be unimportant. Here the optical potential theory can be used reliably. The details of this approximation and its application to various systems are given in several publications [4, 6, 21–28], which the interested reader should consult for further information.

For completeness, we give, in brief, the necessary formulas. In the optical potential approximation, the cross section for radiative decay from a channel with initial state i and potential energy $V_i(R)$ to a channel with final state f and potential energy $V_f(R)$ is

$$\sigma_{fi}(E) = p_i \frac{\pi}{k_i^2} \sum_{J=J_0}^{\infty} (2J+1) [1 - \exp(-4\eta_{fi;J}(E))]. \quad (5)$$

Here p_i is the probability of approach in the initial state i , $E = k^2/2\mu$ is the relative kinetic energy, μ is the reduced mass, and $\eta_{fi;J}(E)$ is the imaginary part of the phase shift. This phase shift is obtained in the distorted-wave approximation by

$$\eta_{fi;J}(E) = \frac{\pi\mu}{2k} \int_0^{\infty} dR |s_{i;J}(kR)|^2 A_{fi}(R), \quad (6)$$

where $k = \sqrt{2\mu[E - V_i(\infty)]}$, and $s_{i;J}(kR)$ is the regular energy normalised solution of the homogeneous radial equation [29]. The quantity,

$$A_{fi}(R) = (4/3)c^{-3} D_{fi}^2(R) |V_f(R) - V_i(R)|^3 \quad (7)$$

is the transition probability. In Eq. (7), $D_{fi}(R)$ is the TDM between the initial and final electronic states. The cross section for collision-induced radiative decay from the entrance channel, i.e., the sum of radiative charge transfer and radiative association, is obtained within the optical potential approximation using Eq. (5).

The rate coefficients $\alpha(T)$, in cm³ s⁻¹ as a function of temperature T (Kelvin), are obtained by averaging the cross section $\sigma_{fi}(E)$ over a Maxwellian velocity distribution and are given by

$$\alpha(T) = \left(\frac{8}{\mu\pi}\right)^{1/2} \left(\frac{1}{k_B T}\right)^{3/2} \int_0^\infty E \sigma_{fi}(E) \exp\left(-\frac{E}{k_B T}\right) dE, \quad (8)$$

where k_B is the Boltzmann constant, $1.380\,648\,52 \times 10^{-23}$ J/K.

We note that the relationship $v\sigma_{fi}(E)$ may be used to designate an effective energy dependent rate $R(E)$, in cm³ s⁻¹ from state f to state i , [27], where $R(E)$ is given by

$$R(E) = \sqrt{2E/\mu} \times \sigma_{fi}(E). \quad (9)$$

This form of the energy dependent quasi-rate may be used to estimate the rate coefficients by converting E to temperature.

3. Results and Discussions

The probability for spontaneous emission, Eq. (7), which drives the radiative charge transfer process, depends on the third power of the photon energy, which for relative kinetic energies less than several eV is approximately the electronic potential energy difference between initial and final states. Thus, we expect that the 3²Π to X²Π and 3²Π to A²Σ⁺ transitions will be the most important, as long as the Franck-Condon overlap between PECs is favourable and the corresponding TDMs are of order unity (in atomic units). As we will show, the calculations support this model. We evaluated Eq. (5) for the 3²Π–X²Π, 3²Π–A²Σ⁺, D²Σ⁻–X²Π, 3²Π–B²Π, and 2⁴Π–b⁴Π transitions. The values of p_i are $\frac{1}{9}$, $\frac{2}{9}$, or $\frac{4}{9}$, respectively, for the initial D²Σ⁻, 3²Σ⁺ or 2⁴Π states. Detailed results for other possible transitions, which we expect to be weaker than the 3²Π to X²Π transition, will be presented in a future publication.

The calculated cross sections are shown in Fig. 3. The 3²Π–X²Π transition is by far the strongest, as expected, followed by the 3²Π–A²Σ⁺ transition. Numerous resonances, typical for ion-atom collisions, occur for collisional energies less than any well depths. Most of the cross sections follow a power law as the energy E decreases, typically, $E^{-1/2}$, though the D²Σ⁻–X²Π cross sections rapidly diminish for energies less than about 0.03 eV, due to the repulsive quadrupole interaction in the D²Σ⁻ initial state. The radiative charge transfer cross sections for the 3²Π–B²Π transition are about 100 times larger than those calculated by Kimura *et al.* [4], but they are still insignificant. Direct charge exchange cross sections were calculated by Kimura *et al.* [3], for energies $E > 10^{-4}$ eV, and these are seen to vary from about 10⁻²¹ cm² at 10⁻⁴ eV to 10⁻¹⁷ cm² at 10 eV, with the D²Σ⁻–B²Π channel the strongest contributor [4], driven by rotational coupling [3]. We expect that radiative charge transfer via the D²Σ⁻–B²Π channel will diminish with energy similarly to the D²Σ⁻–X²Π channel, but because of the smaller magnitude of the TDM, see Fig. 2, it will be relatively weak. Therefore, we conclude for energies less than about 1 eV (11 604.525 Kelvin), radiative charge transfer is more significant than direct charge transfer.

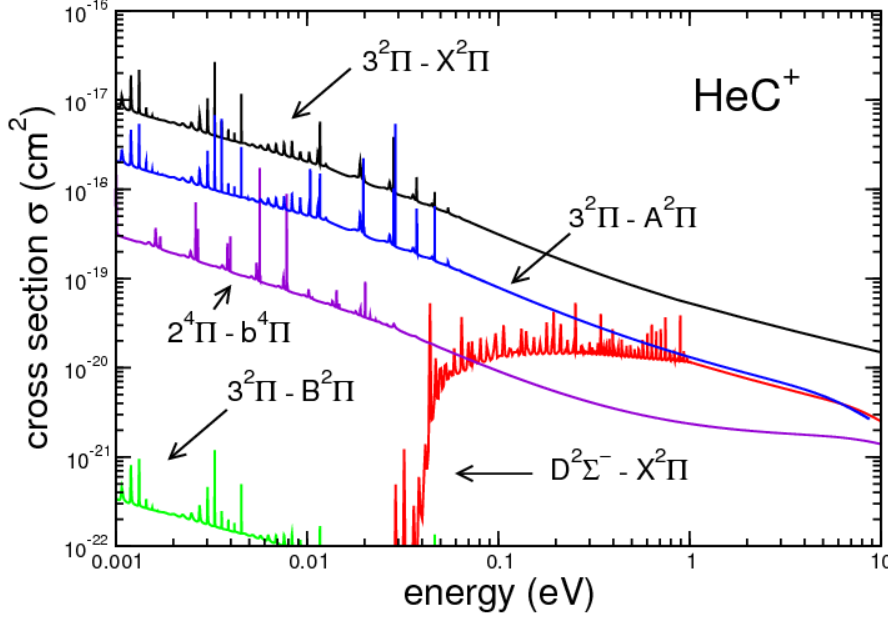


Figure 3. Cross sections (cm^2) for the radiative loss in collisions from the initial channel $\text{C}(^3P) + \text{He}^+(^2S)$ to several of the final channels correlating to states of $\text{C}^+ + \text{He}(1^1S)$. Illustrated are the cross sections σ (cm^2) as a function of the colliding energy E (eV) for the transitions; $3^2\Pi \rightarrow X^2\Pi$ (black line), $3^2\Pi \rightarrow A^2\Pi$ (blue line), $2^4\Pi \rightarrow b^4\Pi$ (violet line), and $3^2\Pi \rightarrow B^2\Pi$ (green line). Dropping off in the middle at $E = 0.03$ eV, is the $D^2\Sigma^- \rightarrow X^2\Pi$ transition (red line).

The rate coefficients for the $\text{C}(^3P) + \text{He}^+(^2S)$ reaction given by Eq. (4) are shown in Fig. 4, for the transitions considered here. The total rate coefficient for radiative charge transfer is about 2×10^{-13} at 10 K, dropping off to about 5×10^{-14} at 10 000 K. In Fig. 4, we also plot the rate coefficients for direct charge transfer from Kimura *et al.* [3], which become larger than the radiative charge transfer process for temperature greater than 3 000 K, approaching 7×10^{-13} at 10 000 K.

In Fig. 5, we compare the radiative charge transfer rate coefficient $\alpha(T)$, calculated using Eq. (8) for the $3^2\Pi$ to $X^2\Pi$ transition, with the radiative charge transfer rate coefficients for $\text{H}^+ + \text{Li}$ [30], $\text{Yb}^+ + \text{Rb}$ [27], $\text{He}^+ + \text{O}$ [6], $\text{He}^+ + \text{H}$ [31], and $\text{He}^+ + \text{Ne}$ [25]. The values for $\text{He}^+ + \text{H}$ from Ref. [31] were multiplied by the factor $\frac{1}{4}$ as noted in Ref. [21]. For $\text{He}^+ + \text{Ne}$ the $B^2\Sigma^+ - X^2\Sigma^+$ cross sections are more than a factor of 10 larger than the $B^2\Sigma^+ - A^2\Pi$ cross sections, so the values in the plot were calculated using the fit from columns 7 and 8 of Table IV of Ref. [25] for the total radiative charge transfer rate coefficients. For $\text{H}^+ + \text{Li}$, which has a repulsive ground state and asymptotic energy difference of about 8 eV between the $2^2\Sigma^+$ and $X^2\Sigma^+$ states, the rate coefficients are comparable to the $3^2\Pi - X^2\Pi$ transition of CHe^+ with an

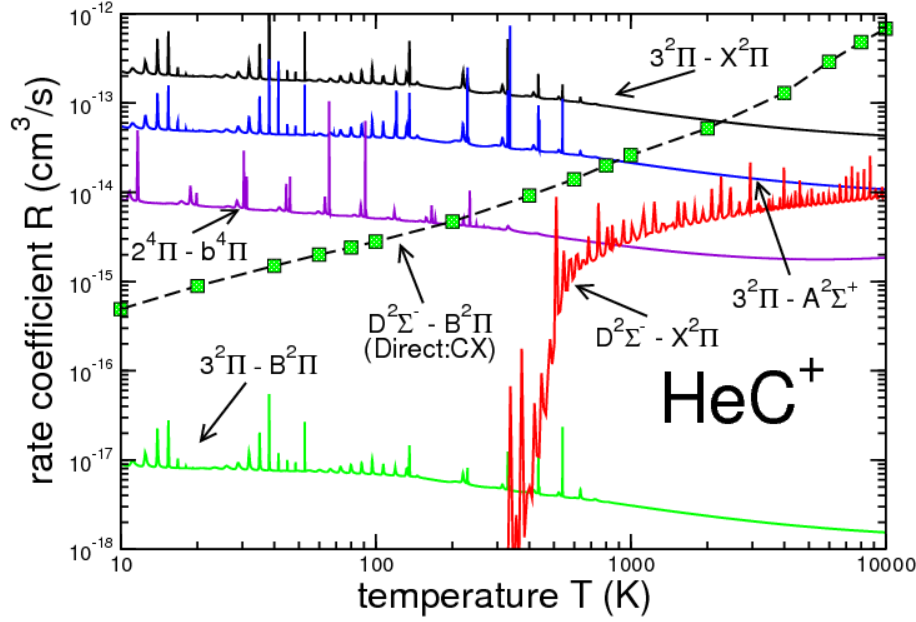


Figure 4. Rate coefficients for radiative loss in collisions from the initial channel $C(^3P) + \text{He}^+(^2S)$ to several of the the final channels correlating to states of $C^+ + \text{He}(1^1S)$. Illustrated are the rate coefficients $R(T)$ (cm^3s^{-1}) as a function of temperature T (K), for the transitions; $3^2\Pi \rightarrow X^2\Pi$ (black line), $3^2\Pi \rightarrow A^2\Sigma^+$ (blue line), $2^4\Pi \rightarrow b^4\Pi$ (violet line), $3^2\Pi \rightarrow B^2\Pi$ (green line), and $D^2\Sigma^- \rightarrow X^2\Pi$ (red line). The dominant $D^2\Sigma^- \rightarrow B^2\Pi$ channel (dashed black line, with green squares) for direct charge exchange (CX) from the work of Kimura et al. [3] is included.

asymptotic energy difference of about 13 eV. The $A^1\Sigma^+ - X^1\Sigma^+$ transition of YbRb^+ has a relatively large TDM [27] compared to the $3^2\Pi$ to $X^2\Pi$ transition of CHe^+ , but the asymptotic energy difference is only about 2 eV and the reduced mass is 20 times larger. For HeH^+ , the $A^1\Sigma^+$ state is highly repulsive and the $X^1\Sigma^+$ state is attractive, leading to comparatively less favorable transition amplitudes compared to the repulsive $3^2\Pi$ and $X^2\Pi$ states of CHe^+ . For HeNe^+ , the ground $X^2\Sigma^+$ state has a shallow well and the asymptotic energy difference for the dominant $B^2\Sigma^+ - X^2\Sigma^+$ transition is 3 eV, compared to about 13 eV for the $3^2\Pi - X^2\Pi$ transition of CHe^+ . The various weight factors (such as we discussed in Sec. 3) for each system, other details of the PECs and TDMS, and the different reduced masses may also contribute to the relative differences between the rate coefficients.

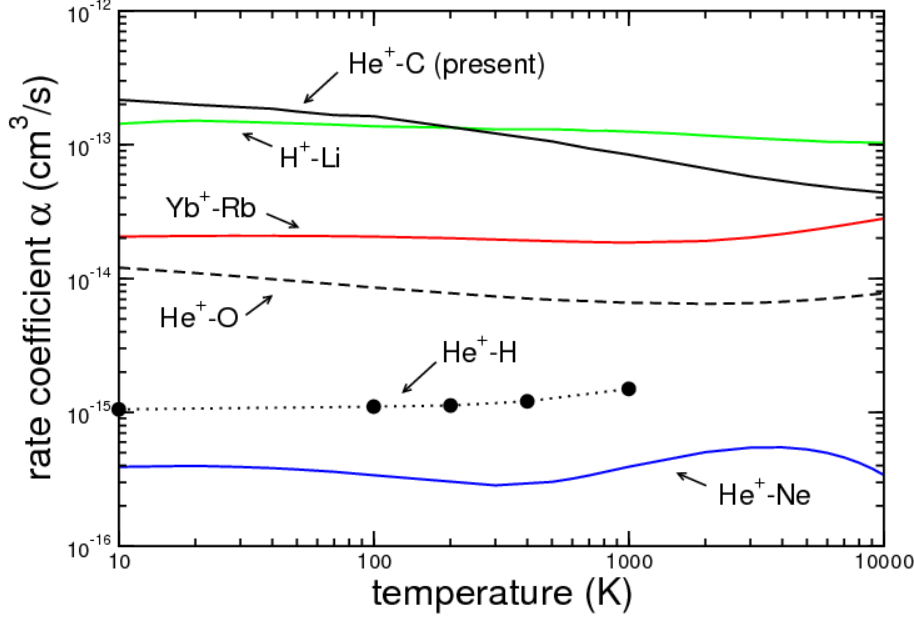


Figure 5. A comparison of rate coefficients, $\alpha(T)$ (cm^3s^{-1}) as a function of temperature $T(K)$, for radiative charge transfer. In order of decreasing magnitude at 10 K, He⁺ and C, $3^2\Pi$ to $X^2\Pi$ transition (black line) present work, H⁺ and Li (green line) [30], Yb⁺ + Rb (red line) [27], He⁺ and O (dashed black line) [6], He⁺ and H [31] (points, connected with dotted line guide), and He⁺ + Ne (blue line) [25]. See text for discussion.

4. Conclusions

From the results of our investigations, we find that radiative charge exchange (RCX) becomes more significant than direct charge exchange (CX) as the relative collisional energy decreases in $\text{C}(^3P) + \text{He}^+$ collisions. Our calculations confirm the earlier finding of Kimura *et al* [4], that radiative charge transfer via the $3^2\Pi\text{-B}^2\Pi$ transition is unimportant. However, similarly to work on $\text{O} + \text{He}^+$, by Zhao and co-workers [6], our results show that radiative charge transfer leaving the residual ion in its ground state is the dominant mechanism. Furthermore, at thermal and lower energies, our results indicate it is much more rapid than direct charge transfer.

Earlier calculated rate coefficients for removal of He⁺(2S) by C or O were found to be too small to affect the ejecta models [3, 6]. We note that charge exchange cross-sections and rates for collisions of Si with He⁺ were considered recently by Satta *et al.* [32] using the multi-channel Landau-Zener approximation (MCLZ). The dominant mechanism is radically different than that for C and O, due to the presence of a manifold of excited states $(\text{SiHe}^+)^*$ above the exit channel energy of Si⁺ in its ground state. However, the calculated rate coefficients are not larger than the estimates of

the 1990's. We note that a similar manifold would be present for the case of charge transfer collisions of S with He⁺, but, to our knowledge, the calculation has not been carried out. Nevertheless, the role of He⁺ in the destruction of CO is affirmed by recent ejecta models [33, 34] and it might be interesting to revisit the models of the 1990's to see if the improved charge exchange rate coefficients now available for C, O, or Si with He⁺ modify the conclusions obtained at that time.

Furthermore, recent models of ejecta chemistry go beyond equilibrium chemistry, but, generally, still suffer from a lack of charge transfer data [35]. The present results might be applicable to modelling the complex interplay of [C II] (or C⁺), C, and CO at the boundaries of interstellar photon dominated regions (PDRs) and in xray dominated regions (XDRs), where the abundance of He⁺ can affect the abundance of CO.

Acknowledgments

We would like to dedicate this work to the late Professor Alexander Dalgarno, FRS, who was a great friend, a true gentleman and a long term mentor to both authors, and from whom we learned a great deal of physics. His sharp intellect and foresight into the solution of problems will be sadly missed by both the AMO and Astrophysics communities. ITAMP is supported in part by a grant from the NSF to the Smithsonian Astrophysical Observatory and Harvard University. B MMcL acknowledges support from the ITAMP visitor's program and from Queen's University Belfast for the award of a Visiting Research Fellowship (VRF). Grants of computational time at the National Energy Research Scientific Computing Center (NERSC) in Berkeley, CA, USA and at the High Performance Computing Center Stuttgart (HLRS) of the University of Stuttgart, Stuttgart, Germany are gratefully acknowledged.

References

- [1] Lepp S, Dalgarno A and McCray R 1990 *Astrophys. J.* **358** 262 URL <http://dx.doi.org/10.1086/168981>
- [2] Liu W, Dalgarno A and Lepp S 1992 *Astrophys. J.* **396** 679 URL <http://dx.doi.org/10.1086/171749>
- [3] Kimura M, Dalgarno A, Chantranupong L, Li Y, Hirsch G and Buenker R J 1993 *Astrophys. J.* **417** 812 URL <http://dx.doi.org/10.1086/173361>
- [4] Kimura M, Dalgarno A, Chantranupong L, Li Y, Hirsch G and Buenker R J 1994 *Phys. Rev. A* **49** 2541 URL <http://dx.doi.org/10.1103/PhysRevA.49.2541>
- [5] Kimura M, Gu J P, Liebermann H P, Li Y, Hirsch G, Buenker R J and Dalgarno A 1994 *Phys. Rev. A* **50** 4854 URL <http://dx.doi.org/10.1103/PhysRevA.50.4854>
- [6] Zhao L B, Stancil P C, Gu J P, Liebermann H P, Li Y, Funke P, Buenker R J, Zygelman B, M Kimura and Dalgarno A 2004 *Astrophys. J.* **615** 1063 URL <http://stacks.iop.org/0004-637X/615/i=2/a=1063>
- [7] Kramida A, Ralchenko Y, Reader J *et al.* 2016 NIST Atomic Spectra Database (version 5.3) National Institute of Standards and Technology, Gaithersburg, MD, USA URL <http://physics.nist.gov/>
- [8] Matoba S, Tanuma H and Ohtsuki K 2008 *J Phys. B: At. Mol. Opt. Phys.* **41** 145205 URL <http://stacks.iop.org/0953-4075/41/i=14/a=145205>
- [9] Tuttle W D, Thorington R L, Viehland L A and Wright T G 2015 *Mol. Phys.* **113** 3767–3782 URL <http://dx.doi.org/10.1080/00268976.2015.1061153>
- [10] Helgaker T, Jorgensen P and Olsen J 2000 *Molecular Electronic-Structure Theory* (New York, USA: Wiley)
- [11] Kendall R A, Dunning Jr T H and Harrison R J 1992 *J. Chem. Phys.* **96** 6796 URL <http://dx.doi.org/10.1063/1.462569>

- [12] Woon D E and Dunning Jr T H 1993 *J. Chem. Phys.* **98** 1358 URL <http://dx.doi.org/10.1063/1.464303>
- [13] Mourik T V, Wilson A K and Dunning Jr T H 1999 *Mol. Phys.* **96** 529–547 URL <http://dx.doi.org/10.1080/002689799165396>
- [14] Werner H J, Knowles P J, Knizia G, Manby F R, Schütz M *et al.* 2015 MOLPRO, version 2015.1, a package of *ab initio* programs, see <http://www.molpro.net>
- [15] Werner H J and Knowles P J 1985 *J. Chem. Phys.* **82** 5053 URL <http://dx.doi.org/10.1063/1.448627>
- [16] Knowles P J and Werner H J 1985 *Chem. Phys. Letts.* **115** 259–267 URL [http://dx.doi.org/10.1016/0009-2614\(85\)80025-7](http://dx.doi.org/10.1016/0009-2614(85)80025-7)
- [17] Grice S T, Harland P W, Maclagan R G A R and Simpson R W 1987 *Int. J. of Mass Spec. Ion. Proc.* **87** 181 URL [http://dx.doi.org/10.1016/0168-1176\(89\)80021-7](http://dx.doi.org/10.1016/0168-1176(89)80021-7)
- [18] Gentry W R and Giese C F 1977 *J. Chem. Phys.* **67** 2355 URL <http://dx.doi.org/10.1063/1.435072>
- [19] Allison D C S, Burke P G and Robb W D 1972 *J. Phys. B: At. Mol. Phys.* **5** 1431–1438 URL <http://dx.doi.org/10.1088/0022-3700/5/8/010>
- [20] Miller J H and Kelly H P 1972 *Phys. Rev. A* **5** 516 URL <http://link.aps.org/doi/10.1103/PhysRevA.5.516>
- [21] Stancil P C and Zygelman B 1996 *Astrophys. J.* **472** 102 URL <http://dx.doi.org/10.1086/178044>
- [22] Stancil P C, Gu J P, Havener C C, Krstic P S, Schultz D R, Kimura M, Zygelman B, Hirsch G, Buenker R J and Bannister M E 1998 *J. Phys. B: At. Mol. Opt. Phys.* **31** 3647 URL <http://stacks.iop.org/0953-4075/31/i=16/a=017>
- [23] Zhao L B, Wang J G, Stancil P C, Gu J P, Liebermann H P, Buenker R J and Kimura M 2006 *J. Phys. B: At. Mol. Opt. Phys.* **39** 5151 URL <http://stacks.iop.org/0953-4075/39/i=24/a=012>
- [24] Liu C H, Qu Y Z, Zhou Y, Wang J G, Li Y and Buenker R J 2009 *Phys. Rev. A* **79** 042706 URL <http://dx.doi.org/10.1103/PhysRevA.79.042706>
- [25] Liu X J, Qu Y Z, Xiao B J, Liu C H, Zhou Y, Wang J G and Buenker R J 2010 *Phys. Rev. A* **81** 022717 URL <http://link.aps.org/doi/10.1103/PhysRevA.81.022717>
- [26] Zygelman B, Lucic Z and Hudson E R 2013 *J. Phys. B: At. Mol. Opt. Phys.* **47** 015301 URL <http://dx.doi.org/10.1088/0953-4075/47/1/015301>
- [27] McLaughlin B M, Lamb H L D, Lane I C and McCann J F 2014 *J. Phys. B: At. Mol. Opt. Phys.* **47** 145201 URL <http://dx.doi.org/10.1088/0953-4075/47/14/145201>
- [28] Shen G, Stancil P C, Wang J G, McCann J F and McLaughlin B M 2015 *J. Phys. B: At. Mol. Opt. Phys.* **48** 105203 URL <http://stacks.iop.org/0953-4075/48/i=10/a=105203>
- [29] Mott, N F and Massey, H S W 1965 *The Theory of Atomic Collisions* 3rd ed (Oxford, UK: Clarendon Press)
- [30] Dalgarno A, Kirby K and Stancil P C 1996 *Astrophys. J.* **458** 397 URL <http://dx.doi.org/10.1086/176823>
- [31] Zygelman B, Dalgarno A, Kimura M and Lane N F 1989 *Phys. Rev. A* **40** 2340 URL <http://dx.doi.org/10.1103/PhysRevA.40.2340>
- [32] Satta M, Grassi T, Gianturco F A, Yakovleva S A and Belyaev A K 2013 *Mon. Not. Roy. Astr. Soc.* **436** 2722 URL <http://dx.doi.org/10.1093/mnras/stt1771>
- [33] Cherchneff I and Dwek E 2009 *Astrophys. J.* **703** 642 URL <http://dx.doi.org/10.1088/0004-637X/703/1/642>
- [34] Clayton D D 2012 *Astrophys. J.* **762** 5 URL <http://dx.doi.org/10.1088/0004-637X/762/1/5>
- [35] Jerkstrand A, Fransson C and Kozma C 2011 *Astron. Astrophys.* **530** A45 URL <http://dx.doi.org/10.1051/0004-6361/201015937>